ASUR—An Airborne SIS Receiver for Atmospheric Measurements of Trace Gases at 625 to 760 GHz

J. Mees, S. Crewell, H. Nett, G. de Lange, H. van de Stadt, J. J. Kuipers, and R. A. Panhuyzen

Abstract—**A heterodyne receiver making use of a SIS waveguide mixer with integrated horn and single backshort tuner has been built. It has been used for a series of airborne measurements of atmospheric trace gases, such as HCl and ClO, above northern Europe during the winter of 1993 and 1994. The receiver is suitable for measurements in the range of 625–760 GHz and shows stable operation in the airplane together with high sensitivity. Best achieved noise temperatures are $T_{\mathrm{DSB}} = 310$ K at 708 GHz in the laboratory and $T_{\mathrm{SSB}} = 1500$ K at 625 GHz for the complete system in the airplane.**

I. Introduction

IN A COLLABORATION between the Laboratory for Space Research (SRON, Groningen) and the Institute of Environmental Physics (Bremen), the former submillimeter atmospheric sounder (SUMAS) [1]–[4] of the University of Bremen has been significantly improved by the use of a SIS junction as detection element instead of the conventional Schottky diode used before. First test flights of the new ASUR (airborne submillimeter SIS radiometer) experiment onboard the German research aircraft FALCON were successfully performed in Dec. 1993. Later, in Feb. 1994 a flight campaign to northern Scandinavia was carried out to measure atmospheric trace gases such as ClO and HCl at the polar vortex. The system shows a significantly reduced overall noise temperature and good stability during flight. Due to this fact, the emission lines of ClO and HCl were measured with high temporal and spatial resolution.

Schottky diodes have been proven to be reliable heterodyne detectors for atmospheric and astronomical receivers over a wide range of frequencies up to several THz. However, Nb-tunnel junctions made out of a sandwich of superconductor-insulator-superconductor (SIS) offer today a significantly better sensitivity and wider bandwidth as nonlinear mixing elements at frequencies up to 750 GHz than any other detector [5]–[8]. They were first used at lower frequencies only. Since then, the frequency range of SIS-mixer receivers has been greatly increased, up to the superconducting gap frequency of Nb and above. This is due to great improvements in precision mechanical engineering, junction fabrication, and in the development of local oscillators for higher frequencies. The higher sensitivity of SIS detectors comes with the disadvantage of lower operating temperatures (L^4He) compared to Schottky diodes. Those can be operated above 20 K where closed cycle coolers are available. This campaign was the first time that an airborne receiver with a SIS tunnel junction mixer has been used for atmospheric measurements of trace gases in the range of 625–686 GHz.

SIS waveguide mixers are being developed at SRON for space applications like FIRST (far-infra-red and submillimeter space telescope). Mixers have been made for 350 GHz [9], and in scaled versions [10] for 500 GHz and 750 GHz. A 1000 GHz mixer is under development. These mixers contain an integrated horn and a single backshort tuner and show a good beam pattern as well as an excellent performance over the whole frequency band of the waveguide. Heterodyne response has been obtained up to 840 GHz. Y-factor measurements in the laboratory show best double sideband noise temperatures of $T_{\mathrm{DSB}} = 310$ K (250 K after correction for the beamsplitter transmission losses) at 708 GHz [11]. The single sideband noise temperature of the complete receiver system is $T_{\mathrm{SSB}} = 1500$ K at 625 GHz and increases with the frequency to 1700 K at 650 GHz as measured during flight.

We will illustrate the sensitivity of our SIS-mixer around the gap frequency and give an overview of the receiver design and its system performance. We will also show results of trace gas measurements during the flight campaigns.

Manuscript received July 28, 1994; revised August 1, 1995. This work was supported in part by the DLR in München and Kiruna, and the ESA under ESTEC Contract 10655/93/NL/SF, and the German Ministry for Research and Technology Contract BMFT 01 LO 9320/0.

J. Mees and H. van de Stadt are with Space Research Organization Netherlands (SRON), 9700 AV Groningen, The Netherlands.

S. Crewell is with the Institute for Environmental Physics, University of Bremen, 28334 Bremen, Germany.

H. Nett was with the Institute for Environmental Physics, University of Bremen, 28334 Bremen, Germany and is presently at ESA/ESTEC, Mission Support, 2200 AG Noordwijk, The Netherlands.

G. de Lange and J. J. Kuipers are with the Department of Applied Physics and Materials Science Centre, University of Groningen, 9747 AG Groningen, The Netherlands.

R. A. Panhuyzen was with the Space Research Organization Netherlands (SRON), 9700 AV Groningen, The Netherlands. He is now with the Department of Applied Physics and Materials Science Centre, University of Groningen, 9747 AG Groningen, The Netherlands.

IEEE Log Number 9414838.

II. Experiment Description

$Nb/Al_2O_3/Nb$-tunnel junctions produced at SRON have an area of about 1 μm^2 and are fabricated with a selective niobium over-etch process (SNOEP) [12] on 2″ quartz wafers. The dimensions of a single quartz substrate suitable for the 750 GHz waveguide mixer block are $(50\times80\times4200)$ μm^3. The normal state resistance R_N of a junction is usually between 10–20 Ω and the specific capacitance $C_J = 55\ fF/\mu m^2$. The device used in the airplane measurements has two junctions in series and a normal state resistance of $R_N = 42$ Ω. The Josephson critical current density is $\sim 12\ kA/cm^2$ and $R_N/R_S \sim 18$, where R_S is the subgap resistance at 2 K physical temperature.

0018–9480/95$04.00 © 1995 IEEE

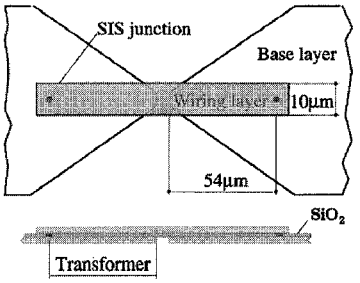

Fig. 1. Quartz chip with SIS-junction, tuning network, and low-pass filter.

The mixer described here consists of a full-height waveguide measuring $300\times150\mu m^2$, with a single backshort and an integrated diagonal horn. The mixer is mounted in a L^4He bath dewar with rigid support system. The noncontacting backshort has two $\lambda/4$ choke sections with a high and a low impedance. The quartz chip with the junction lies across the waveguide in the substrate channel which measures (100×100) μm^2 in the cross section. It contains an on-chip low-pass filter with six alternating $\lambda/4$ high-low impedance sections on each side. This prevents signal currents from leaking into the substrate channel. A superconducting magnet made of Nb-Ti wire is used to suppress the Josephson effects.

Embedded in a matching and transforming network made out of superconducting microstrips, the junction impedance can be matched to the waveguide impedance over a broad range of frequencies. We have successfully designed and fabricated several kinds of integrated tuning structures for different frequency regimes and bandwidths using SIS tunnel junctions as detectors. We studied the frequency response of waveguide mixers by means of a Fourier transform spectrometer of the Michelson type [13]. The bandwidth varies with the type of tuning network and can be as large as 170 GHz at a central frequency of 670 GHz. Heterodyne experiments show that one-step transformers are most suitable for our purposes. This simple design, shown in Fig. 1, offers not only a broadband power coupling to the junction but also low losses at frequencies below 700 GHz, which results in a high sensitivity of the mixer. It has been shown that transformer designs are most appropriate not only for SIS junctions, but also for other detectors and environments. Two-step transformers offer up to 30% bandwidth in antenna-coupled designs. Complete on-chip filter structures with bandpass characteristics, e.g., Chebyshev filters, made out of superconducting striplines are possible [14].

Fig. 2 shows a simple equivalent electronic RF circuit of a SIS junction and the surrounding waveguide. The junction is represented by the geometrical capacitance C, the nonlinear admittance G_{RF}, and the susceptance B_{RF}. The last two are caused by internal quantum effects. The transformer network is represented by a lossy microstrip line with the characteristic admittance Y_0 and electrical length γ. The superconducting microstrip designs were calculated by means of the Mattis–Bardeen theory [15]. The admittance of the waveguide is assumed to be real and the effect of the backshort purely imaginary.

Fig. 3 shows the video response of three different samples obtained with a Michelson spectrometer. The spectral response

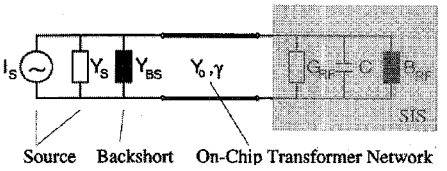

Fig. 2. Equivalent RF-circuit of the junction and environment.

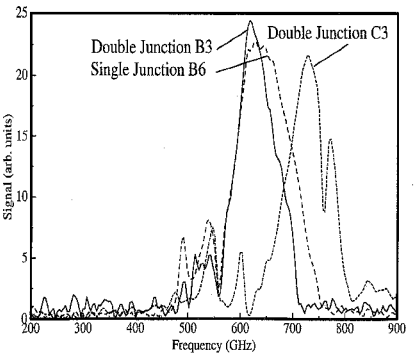

Fig. 3. FTS response of samples B3, B6, and C3 with different lengths of the single-step transformer.

indicates the power coupling to the SIS junction in the waveguide influenced by the backshort and the integrated tuning network. Samples B3 and B6 make use of single-step transformers, 10 μm wide and 54 μm long, as integrated matching network. The single junction element B6 shows a broad 3dB-bandwidth of about 125 GHz and sample B3 (Fig. 1) with two junctions in series with 90 GHz a somewhat smaller bandwidth. Both samples have the same resonance frequency of about 640 GHz. The transforming microstrip of sample C3 has a width of 10 μm and a length of 49 μm which results in a higher resonance frequency of 720 GHz. Since the Michelson measurements are influenced by the position of the backshort, the expression "resonance frequency" has to be interpreted with care. We have investigated a whole set of measurements for each sample with different backshort positions. The curves shown in Fig. 3 represent the central figures of the measurement sets. Absorption lines in the spectra, e.g., at 557 and 752 GHz, are due to water vapor in the spectrometer, which was not evacuated.

The frequency range of interest for the flight campaign was between 625 and 686 GHz. Laboratory heterodyne tests showed a slightly superior performance of sample B3 above the other. Therefore, sample B3 was used during all further laboratory tests and flight experiments. Fig. 4 shows its DC IV-curves, unpumped and pumped by the local oscillator at 680 GHz, together with the IF heterodyne response arising from hot (300K) and cold (80K) loads in front of the receiver. The IF response shows also some remaining structures of the Josephson effect that could not be suppressed completely by the applied magnetic field. The reason for this might be that we used a two-junction array where both junctions are not completely identical. The gap voltage of this sample was V_{gap} =2.55 mV at 4.2 K, corresponding to a gap frequency of f_{gap} = 616 GHz. Cooling in the laboratory to 2 K increased the gap voltage to 2.65 mV and the gap frequency

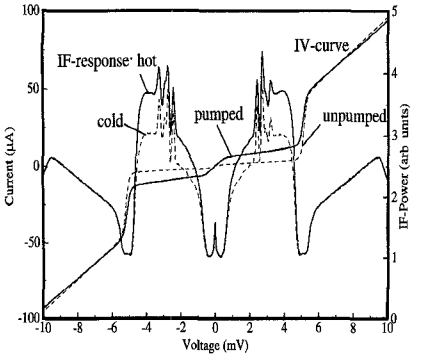

Fig. 4. Pumped and unpumped IV-curve of sample B3 with hot (300K) and cold (77K) IF response at 680 GHz.

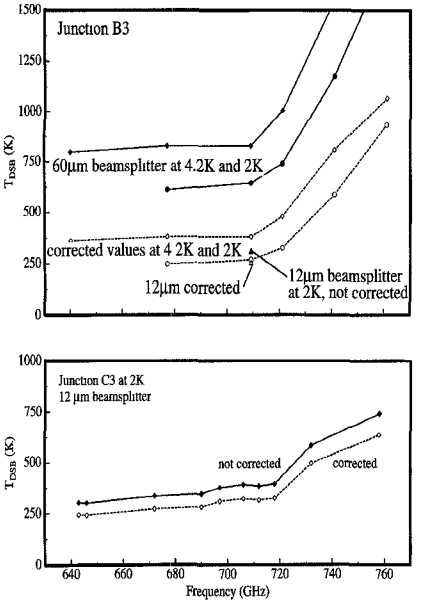

Fig. 5. (Top graph) Double sideband noise temperature of sample B3 for different operating temperatures and frequencies including beamsplitter losses. The lower curves represent the resulting noise temperatures when the losses are excluded. (Bottom graph) T_{DSB} of sample C3 at 2K.

to $f_{\mathrm{gap}} = 640$ GHz, respectively. This means that almost all measurements were done at frequencies which clearly exceeded the gap frequency of this specific sample. We believe that the performance of the receiver can be improved by using a sample with higher gap voltage.

Fig. 5 shows the laboratory heterodyne performance of sample B3 and C3 characterized by the double sideband noise temperature T_{DSB} for different operating temperatures and frequencies. In the top graph of Fig. 5, the two upper curves show measurements with a mylar beamsplitter of 60 μm thickness at 4.2 and 2 K He bath temperature. Curves that are corrected for the losses of the beamsplitter are shown below. To verify these corrections, a measurement with a 12 μm thick beamsplitter was investigated. This measurement yielded $T_{\mathrm{DSB}} = 310$ K at 708 GHz at 2 K physical temperature. The corrected value of this measurement is 250 K and lies within 5 K of that of the measurement with the 60 μm thick beamsplitter. In the beginning Y-factor measurements were usually performed with a 60 μm thick beamsplitter. Only at a single strong line of the carcinotron measurements were undertaken with the thin beamsplitter. Later, the optical set-up was improved and measurements at a wide range of frequencies were done. The bottom graph of Fig. 5 shows the performance of sample C3 at 2 K measured with the 12 μm thick mylar beamsplitter. The tuned heterodyne bandwidth of both samples is rather wide ranging at least from 640 to 760 GHz. Below 640 GHz, measurements to determine the whole bandwidth were not possible due to the lack of suitable local oscillators. At 625 GHz only the single sideband noise temperature could be determined in the flight set-up.

The mylar beamsplitters used in the measurements are 60 μm and 12 μm thick. Mylar has a dielectric constant of 1.73 which results in calculated transmissions of 56.5% and 91.5% at 710 GHz. Transmission measurements are in good agreement the calculations and show $T = 60\%$ and 90%, respectively. These values were used for the corrections.

III. The Optical Layout

The atmospheric signal enters the airplane through a HDPE window [16], especially designed for that frequency range to avoid standing wave problems. This wedged window is 200 mm in diameter, 13 mm thick on one side and 14 mm on the other side. The difference in the traveling lengths across the window surface reduces the frequency dependent variation of the transmission loss of plane parallel plates due to the Fabry–Perot effect.

A rotating mirror points in an alternating cycle to the window and to calibration loads at 300 and 77 K. A roof-top pathlength modulator serves to eliminate the remaining standing wave problems. Two Martin–Puplett type interferometers are used as a single sideband filter (SSB) and as a diplexer in order to combine the atmospheric and the LO signal. A combination of an elliptical mirror and a cooled high-density polyethylene (HDPE) lens in front of the mixer determines the optical system. Antenna pattern measurements indicate that the performance of the cold lens does not change significantly from 300K to 4.2K. The complete optical system was calculated with Gaussian beam optics to minimize losses in the optical system. Since the aperture diameter of most optical components is 50 mm, the optical system is designed to have a maximum beam radius smaller than 12.5 mm along the optical path. The asymptotic angle of growth of the receiver beam radius is 0.7°.

The LO power requirement of a SIS junction is much smaller than that of a Schottky diode and the LO used emitted far more power than necessary for a SIS junction. We therefore implemented in the LO path a polarizing wiregrid that can be rotated to attenuate the signal. This grid is located between the LO and the signal path entry. The dewar window is made of 200 μm thick mylar sheet. In addition a 110 μm thick SiO_2 plate is mounted on the 77 K radiation shield and serves as low-pass filter. An additional wire grid is mounted inside the dewar in front of the mixer block to dump the cross-polarization signal on a cooled absorber at 4.2 K. Fig. 6 shows a schematic layout of the optics.

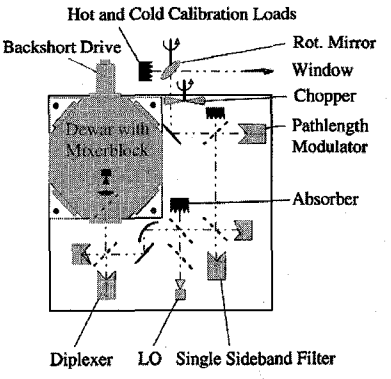

Fig. 6. Schematic layout of the quasi-optics.

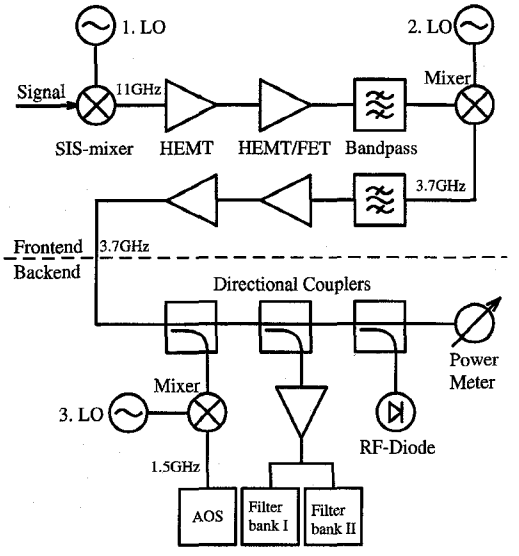

Fig. 7. IF chain of the receiver.

IV. The IF System

The electrical layout of the receiver system is shown in Fig. 7. Two solid state oscillators [17] served for the different frequency bands as local oscillators (1^{st} LO) and were exchanged in various flights. One operated at 637–639 GHz to serve the lower frequency bands while the other radiated at 675 GHz for the higher frequency bands. The IF frequency was chosen to be 11.08 GHz, to cover several interesting molecular lines with both sidebands. Switching between measurements of those lines was done by adjusting the single sideband filter (SSB).

The mixer IF output was coupled through a commercial bias tee and an isolator directly to the first IF amplifier. The first stage was a low-noise HEMT amplifier [18] that was mounted inside the dewar on the 4 K stage. The noise temperature of this amplifier is below 15 K for the whole frequency band, from 10–12 GHz. The IF signal was further amplified and filtered before it was mixed down a second time.

The second IF output toward the backend is centered at $f_{IF} = 3.7$ GHz with a bandwidth of 1200 MHz. The power level varies between 0 and 10 dBm. The backend consists of an acousto-optical spectrometer (AOS), two filter banks, and a UNIX system for the data retrieval. The power is distributed via directional couplers to the spectrometers and sensors that register the power level. The fast detector, a Schottky diode, was used for bias sweeps to optimize the SIS mixer. The slower sensor is a power meter whose measurements were taken permanently as housekeeping data by the computer system.

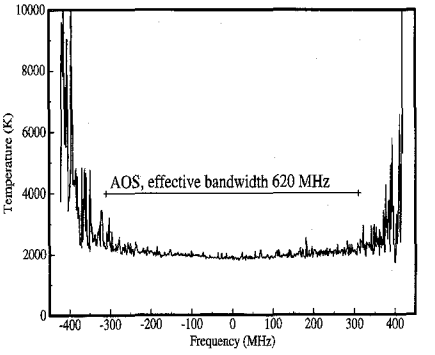

Fig. 8. System noise temperature over the AOS bandwidth. For data analysis the outer channels are not taken into account, because of the higher noise level there.

The filter banks have a central frequency of 3.7 GHz with 28 channels and a bandwidth of 1200 MHz. The channel bandwidth is 8 MHz in the center and increases to 80 MHz at the edge of the band. This is done to cover a large bandwidth with a small number of channels, while simultaneously obtaining a high resolution in the center.

The AOS covers about 880 MHz containing 2000 channels with an effective resolution of 1.4 MHz. Fig. 8 shows the system noise temperature over the AOS bandwidth. For data analysis the bandwidth is restricted to 620 MHz where the noise temperature was relatively constant. In Fig. 8 four channels are coadded to give one data point to increase the signal to noise ratio. This results in an effective resolution of 2.8 MHz. The outer channels are not taken into account, because of their higher noise level.

The UNIX system is used to control important parts, e.g., the rotating mirror, of the experiment and to retrieve the data. It stores the data on tape together with housekeeping data from various sensors and gives an online quick-look at the obtained data and spectra.

V. Measurement Campaign

The receiver system was built into a Falcon aircraft operated by the German space agency DLR in Oberpfaffenhofen. During the winter 1993 and 1994, a total of eight observation flights were made, five solely in an observation campaign to Kiruna in northern Sweden and above the polar sea. The flight campaign to Kiruna covered the time from Feb. 7 to 18, 1994. The typical flight time was about 2.5-3 h and covered a distance of about 2000 km. Typical flight altitude for measurements was 34000–37000 feet and the optical depth along the line of sight is $\tau = (2 \pm 0.5) \cdot 10^{-3}$. This is at a Zenith angle of 78° and at a height of 36000 ft. The instrument records the data from the beginning of the flight although spectral lines are measurable at higher altitudes only depending on the line strength and the meteorological

TABLE I
MEAN SINGLE SIDEBAND SYSTEM NOISE TEMPERATURE OF THE COMPLETE RECEIVER FOR DIFFERENT MOLECULES OVER THE MEASURED FREQUENCY BAND OF 1200 MHz. THIS BANDWIDTH IS DETERMINED BY THE FILTER BANK

Molecule	Frequency [GHz]	T_{SSB} [K]
HCl	625.913±0.6	1500
N_2O	627.286±0.6	1500
O_3	648.073±0.6	1900
ClO	649.448±0.6	1700
O_3	664.300±0.6	1950
ClO	686.460±0.6	2300

conditions. Measurements of four different molecules were made at six frequencies ranging from 625–686 GHz as listed in Table I.

The flights were coordinated for comparison of the data with other experiments, such as the balloon borne submillimeter limb sounder (SLS) of the Jet Propulsion Laboratory, the microwave limb sounder (MLS) experiment on-board the upper atmospheric research satellite (UARS) satellite and a German research aircraft (Transall). The Transall contained several instruments for trace gas measurements, such as O_3, $ClONO_3$, and HNO_3.

VI. SYSTEM PERFORMANCE

The overall single sideband system noise temperature measured continuously by the power meter compare well with the noise fluctuations observed on single channels of the AOS and the filter banks. During a typical flight, several molecules were measured. Switching from the upper to the lower sideband was done by tuning the SSB filter. The observation of ClO and HCl in a single flight was of greatest interest and made it necessary to tune the LO to a new frequency. In either case, the optimization of SIS bias voltage, backshort and diplexer position, and LO power level was necessary. In general, tuning to a new frequency band takes about 5 to 10 minutes.

The noise temperatures achieved for the different molecular lines are shown in Table I. Since the receiver had to be tuned in a relatively short time, the listed numbers may not represent the lowest reachable noise temperatures. The system noise temperature increases, as expected, toward higher frequencies. The over-all single sideband noise temperatures T_{SSB} given in Table I are somewhat higher than the laboratory measurements in Fig. 5. To compare both type of measurements the double sideband noise temperature T_{DSB} has to be doubled and 300 K added for the warm sideband termination which was located inside the aircraft. Because the laboratory measurements have been performed using a simple set-up the residual differences can be explained by losses due to polarization selection and in the optical system. Also, the laboratory measurements were done at a somewhat lower physical temperature of 2 K instead of 2.9 K in the airplane.

VII. MEASUREMENTS

To obtain the submillimeter emission spectra, the raw data were calibrated with the measurements of the hot and cold calibration load. They were corrected for the window transmission losses and integrated to obtain a sufficiently high signal to noise ratio. Only spectra above 30 000 feet with a roll angle lower than three degrees and a stable power level were used. Figs. 9 and 10 show as an example the spectrum of HCl with an integration time of 630 seconds together with a calculated *a priori* spectrum at 625 GHz. Differences in the power levels of the measured and calculated spectra are due to different water vapor levels. The spectrum of ClO at 649 GHz was integrated during 562 sec and exhibits an amplitude of ~1.5 K (Fig. 11). There is also some indication for an additional, weak $^{18}O_3$ line in the vicinity of ClO.

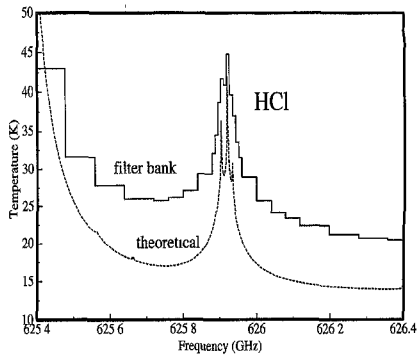

Fig. 9. Synthetic and measured spectra of HCl at $f = 625.9168$ GHz measured on Feb. 15, 1994. The integration time is 630 seconds and the rms error 0.07 K.

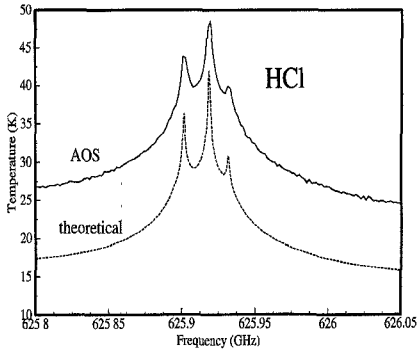

Fig. 10. Synthetic and measured spectra of HCl at $f = 625.9168$ GHz measured on Feb. 15, 1994. The integration time is 630 seconds and the rms error 0.07 K.

VIII. CONCLUSION

The application of a SIS tunnel junction mixer in airborne measurements has been successfully demonstrated in the frequency range from 625 to 686 GHz. The sensitivity compared to the former Schottky detector is about three times higher. The broadband response up to 760 GHz is due to the use of an integrated tuning network with a single-step microstrip transformer. During a series of eight flights in winter 1993 and 1994, measurements of four different molecules at six different frequency bands could be performed with high spectral and spatial resolution. The lowest noise temperatures so far achieved are about $T_{DSB} = 310$ K at 708 GHz in the laboratory and $T_{SSB} = 1500$ K at 625 GHz for the complete receiver system in the airplane. This successful campaign

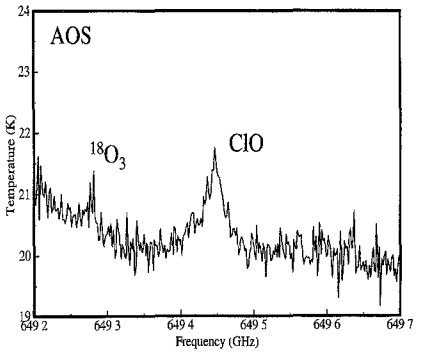

Fig. 11. AOS spectrum of ClO at $f = 649.448$ GHz measured on Feb. 15, 1994. The integration time is 562 seconds and the rms error 0.1 K.

has shown that airborne measurements using an appropriate extremely low-noise receiver is a convenient technique for fast and accurate investigation of trace gases in situations of disturbed atmospheric chemistry.

ACKNOWLEDGMENT

The authors would like to acknowledge the help and support in the measurements and for the flight campaign of A. Baryshev, H. Golstein, W. Horinga, U. Klein, H. Küllmann, G. Naeveke, D. Nguyen, H. Schaeffer, J. Urban, and J. Wezelman. We thank B. Franke, J. Wohlgemuth, T. Wehr, and J. Langen who participated in the data analysis and program development. An important part of this work, the development of the SIS mixer, is based on the mixer work and filter design of C. E. Honingh. We thank P. Hartogh from the Max-Planck-Institut für Aeronomie for the loan of a filter bank. We acknowledge the continuous assistance of K. Künzi, T. de Graauw, and E. Armandillo.

REFERENCES

[1] H. Nett, S. Crewell, U. Klein, and J. Langen, "Submillimeter-wave radiometry," *European Polar Ozone Workshop*, Schliersee, FRG, Oct. 1990, Air Pollution Res. Rep 34. ISBN 2-87263-060, pp. 81–84, 1990.

[2] H. Nett, S. Crewell, and K. Künzi, "Heterodyne detection of stratospheric trace gases at submillimeter-wave frequencies," *Int. Geoscience and Remote Sensing Symp.*, Helsinki, Finland, 1991, IEEE no. 91CH2971-0, vol. 1, pp. 201–204, 1991.

[3] ——, "A 625–650 GHz heterodyne receiver for airborne operation," in *16th Int. Conf. Infrared and Millimeter Waves*, Conf. Dig., SPIE vol. 1576, 1991, pp. 460–461.

[4] S. Crewell, P. Hartogh, K. Künzi, H. Nett, and T. Wehr, "Aircraft measurements of ClO and HCl during EASOE 1991/92," *Geophys. Res. Letters*, Special Issue on EASOE, to be published.

[5] J. Zmuidzinas, H. G. LeDuc, J. A. Stern, and S. R. Cypher, "Two-junction tuning circuits for submillimeter SIS mixers," *IEEE Trans. Appl. Superconductivity*, vol. 42, pp. 668–671, 1994.

[6] J. W. Kooi, C. K. Walker, H. G. LeDuc, T. R. Hunter, D. J. Benford, and T. G. Philips, "A low noise 665 GHz SIS quasiparticle waveguide receiver," submitted to *IEEE Trans. Microwave Theory Tech.*

[7] M. Salez, P. Febvre, W. R. McGrath, B. Bumble, and H. G. LeDuc, "An SIS waveguide heterodyne receiver for 600–635 GHz," *Int. J. Infrared Millimeter Waves*, vol. 15, no. 2, pp. 349–369, 1994.

[8] A. I. Harris, K -F. Schuster, R. Genzel, B. Plathner, and K.-H. Gundlach, "FANATIC: An SIS radiometer for radio astronomy from 660 to 690 GHz," *Int. J. Infrared Millimeter Waves*, vol. 15, no. 9, pp. 1465–1480, 1994.

[9] C. E. Honingh, G. de Lange, M. M. T. M. Dierichs, H. H. A. Schaeffer, T. de Graauw, and T. M. Klapwijk, "Performance of a two-junction array SIS mixer operating around 345 GHz," *IEEE Trans. Microwave Theory Tech.*, vol. 41, no. 4, pp. 616–623, 1993.

[10] G. de Lange, C. E. Honingh, J. J. Kuipers, H. H. A. Schaeffer, R. A. Panhuyzen, T. M. Klapwijk, and H. van de Stadt, and M. W. M. de Graauw, "Heterodyne mixing with Nb tunnel junctions above the gap frequency," *Appl. Phys. Lett.*, vol. 64, pp. 3039–3042, 1994.

[11] J. Mees, G. de Lange, A. Skalare, C. E. Honingh, S. V. Shitov, R. A. Panhuyzen, H. van de Stadt, T. de Graauw, and T. M. Klapwijk, "SIS mixers around the gap frequency," in *Int. Conf. Millimeter and Submillimeter Waves and Applications Conf Dig.*, SPIE, vol. 2250, 1994, pp. 413–414.

[12] M. M. T. M. Dierichs, R. A. Panhuyzen, C. E. Honingh, M. J. de Boer, and T. M. Klapwijk, "Submicron niobium junctions for submillimeter-wave mixers," *Appl. Phys. Lett.*, vol. 62, pp. 774–776, 1993.

[13] Qing Hu, C. A. Mears, P. L. Richards, and F. L. Lloyd, "Measurements of integrated tuning elements for SIS mixers with a Fourier transform spectrometer," *Int. J. Infrared Millimeter Waves*, vol. 9, no. 4, pp. 303–320, 1988.

[14] J. Mees, M. Nahum, and P. L. Richards, "New designs for antenna-coupled superconducting bolometers," *Appl. Phys. Lett.*, vol. 59, no. 18, 1991.

[15] R. L. Kautz, "Picosecond pulses on superconducting striplines," *J. Appl. Phys.*, vol. 49, no 1, pp. 308–314, 1978.

[16] S. Crewell, "Submillimeter-Radiometrie mit einem flugzeuggetragenen Empfänger zur Messung atmosphärischer Spurengase," Ph.D. dissertation, Shaker, Aachen, 1993, ISBN 3-86111-674-X.

[17] Radiometer Physics, Bergerwiesen Straße 15, 53340 Meckenheim, Germany.

[18] Berkshire Technologies, Inc., 5427 Telegraph Ave, Oakland, CA USA.

J. Mees, photograph and biography not available at the time of publication.

S. Crewell, photograph and biography not available at the time of publication.

H. Nett, photograph and biography not available at the time of publication.

G. de Lange, photograph and biography not available at the time of publication.

H. van de Stadt, photograph and biography not available at the time of publication.

J. J. Kuipers, photograph and biography not available at the time of publication.

R. A. Panhuyzen, photograph and biography not available at the time of publication.